

NLO corrections to the hard Pomeron behavior of the charm structure functions

$F_k^c(k = 2, L)$ at low- x

G.R.Boroun* and B.Rezaei†

Physics Department, Razi University, Kermanshah 67149, Iran

(Dated: June 13, 2021)

We show that the charm structure functions F_k^c have a hard pomeron behavior at low- x , as the gluon distribution is dominated by the hard (Lipatov) pomeron at small x and all Q^2 values. It is shown that the charm structure functions obtained, using the gluon distribution functions, are in agreement with data from HERA in the next-to-leading analysis (NLO). Having checked that this behavior gives the charm structure functions exponent independent of x . With respect to the hard (Lipatov) pomeron for the low x gluon distribution, we provide a compact formula for the ratio $R^c = F_L^c/F_2^c$ that is approximately independent of x at low- x and its independent of the input gluon distribution function at all Q^2 values.

Introduction

The small- x region of the deep inelastic scattering (DIS) offers a unique possibility to explore the Regge limit of perturbative quantum chromodynamics (PQCD) [1,2]. This theory is successfully described by the exchange of a particle with appropriate quantum numbers and the exchange particle is called a Regge pole. Phenomenologically, the Regge pole approach to deep inelastic scattering implies that the structure functions are sums of powers in x . As the simplest fit to the small x data corresponds to $F_2(x, Q^2) = \sum_i A_i(Q^2)x^{-\lambda_i}$, where the singlet part of the structure function is controlled by pomeron exchange at small x . HERA shows, this behavior for the gluon and sea quark distributions at small x . As, in the limit $x \rightarrow 0$, the gluon distribution will become large, so its contribution to the evolution of the parton distribution becomes dominant. Therefore the gluon distribution has a rapid rise behavior at small x as

$$xg(x, Q^2) = A_g x^{-\lambda_g}, \quad (1)$$

where λ_g is the pomeron intercept minus one. This steep behavior of the gluon generates a similar steep behavior of F_k^c at small x . Because the gluon will drive the quark singlet distribution, so that the charm structure functions F_k^c is expected to rise approximately like a power of x . For $Q^2 \leq 1 \text{ GeV}^2$, the simplest Regge phenomenology predicts that the value of $\lambda_S = \alpha_P(0) - 1 \simeq 0.08$ is consistent with the hadronic Regge theory [3-5] where $\alpha_P(0)$ is described soft pomeron dominant with its intercept slightly above unity (~ 1.08). Whereas for $Q^2 \geq 1 \text{ GeV}^2$ the slope rises steadily to reach a value greater than 0.3 by $Q^2 \approx 100 \text{ GeV}^2$ where hard pomeron is dominant. This larger value of λ_S is not so far from that expected using BFKL [6] ideas. There are some other authors [3-5]

who extended their Regge model adding a hard Pomeron with intercept 1.44, which allows them to describe the low x HERA data up to Q^2 values of a few hundred GeV^2 . HERA data for the charm structure functions $F_k^c(x, Q^2)$, ($k = 2, L$), over a wide range of Q^2 , require only a hard pomeron as the coupling of the soft pomeron to charm is apparently very small. The charm structure function can be described by a single power of x

$$F_k^c(x, Q^2) = A_k^c x^{-\lambda_k^c}, \quad (2)$$

where λ_k^c is pomeron exponent and we expect to determine. The study of production mechanisms of heavy quarks provides us with new tests of QCD. As in perturbative QCD (pQCD) physical quantities can be expanded in the strong coupling constant $\alpha_s(\mu^2)$. When the scale μ has to be large, provided we are dealing with so called hard processes. In the case of heavy quark production, we can have condition that the heavy quarks produced from the boson- gluon fusion (BGF) according to Fig.1. That is, in PQCD calculations the production of heavy quarks at HERA proceeds dominantly via the direct BGF, where the photon interacts indirectly with a gluon in the proton by the exchange of a heavy quark pair [7-13]. In the BGF dynamic, the charm (beauty) quark is treated as a heavy quark and its contribution is given by fixed- order perturbative theory. With respect to the recent measurements of HERA, the charm contribution to the structure function at small x is a large fraction of the total [14-15], as this value is approximately 30% (1%) fraction of the total. This behavior is directly related to the growth of the gluon distribution at small x . We know that the gluons couple only through the strong interaction, consequently the gluons are not directly probed in DIS. Only contributing indirectly is via the $g \rightarrow q\bar{q}$ transition. This involves the computation of the BGF process $\gamma^* g \rightarrow c\bar{c}$. This process can be created when the squared invariant mass of the hadronic final state has the condition that $W^2 \geq 4m_c^2$. In this paper, we investigate the hard (Lipatov) Pomeron

*Electronic address: grboroun@gmail.com; boroun@razi.ac.ir

†brezaei@razi.ac.ir

behavior of the charm structure functions and present the ratio of the $R^c = \frac{F_L^{cc}}{F_2^{cc}}$ with respect to this behavior which is independent of the input gluon distribution function.

Charm Structure Functions

In the low- x range, where only the gluon contribution is matter, the charm quark contribution $F_k^c(x, Q^2, m_c^2)$ ($k = 2, L$) to the proton structure function is given by this form

$$F_k^c(x, Q^2, m_c^2) = 2e_c^2 \frac{\alpha_s(\mu^2)}{2\pi} \int_{1-\frac{1}{a}}^{1-x} dz C_{g,k}^c(1-z, \zeta) \times G\left(\frac{x}{1-z}, \mu^2\right), \quad (3)$$

where $a = 1 + 4\zeta(\zeta \equiv \frac{m_c^2}{Q^2})$, $G(x, \mu^2)$ is the gluon distribution function and μ is the mass factorization scale, which has been put equal to the renormalization scales $\mu^2 = 4m_c^2$ or $\mu^2 = 4m_c^2 + Q^2$. Here $C_{g,k}^c$ is the charm coefficient functions in LO and NLO analysis as

$$C_{k,g}(z, \zeta) \rightarrow C_{k,g}^0(z, \zeta) + a_s(\mu^2)[C_{k,g}^1(z, \zeta) + \bar{C}_{k,g}^1(z, \zeta) \ln \frac{\mu^2}{m_c^2}], \quad (4)$$

where $a_s(\mu^2) = \frac{\alpha_s(\mu^2)}{4\pi}$ and in the NLO analysis

$$\alpha_s(\mu^2) = \frac{4\pi}{\beta_0 \ln(\mu^2/\Lambda^2)} - \frac{4\pi\beta_1}{\beta_0^3} \frac{\ln \ln(\mu^2/\Lambda^2)}{\ln(\mu^2/\Lambda^2)} \quad (5)$$

with $\beta_0 = 11 - \frac{2}{3}n_f$, $\beta_1 = 102 - \frac{38}{3}n_f$ (n_f is the number of active flavours).

In the LO analysis, the coefficient functions BGF can be found [16], as

$$C_{g,2}^0(z, \zeta) = \frac{1}{2}([z^2 + (1-z)^2 + 4z\zeta(1-3z) - 8\zeta^2 z^2] \times \ln \frac{1+\beta}{1-\beta} + \beta[-1 + 8z(1-z) - 4z\zeta(1-z)]), \quad (6)$$

and

$$C_{g,L}^0(z, \zeta) = -4z^2\zeta \ln \frac{1+\beta}{1-\beta} + 2\beta z(1-z), \quad (7)$$

where $\beta^2 = 1 - \frac{4z\zeta}{1-z^2}$.

At NLO, $O(\alpha_{em}\alpha_s^2)$, the contribution of the photon-gluon component is usually presented in terms of the coefficient functions $C_{k,g}^1, \bar{C}_{k,g}^1$. Using the fact that the virtual photon-quark(antiquark) fusion subprocess can be neglected, because their contributions to the heavy-quark leptonproduction vanish at LO and are small at NLO [6,17]. In a wide kinematic range, the

contributions to the charm structure functions in NLO are not positive due to mass factorization. Therefore the charm structure functions are dependence to the gluonic observable in LO and NLO. The NLO coefficient functions are only available as computer codes[17,18]. But in the high-energy regime ($\zeta \ll 1$) we can use the compact form of these coefficients according to the Refs.[18,19].

Exploiting the low- x behavior of the gluon distribution function according to the hard (Lipatov) Pomeron as

$$G(x, \mu^2) \rightarrow x^{-\lambda_g}. \quad (8)$$

The power of λ_g is found to be either $\lambda_g \simeq 0$ or $\lambda_g \simeq 0.5$. The first value corresponds to the soft Pomeron and the second value to the hard (Lipatov) Pomeron intercept. Based on the hard (Lipatov) pomeron behavior for the gluon distribution, let us put Eq.(8) in Eq.(3). After doing the integration over z , Eq.(3) can be rewritten as

$$F_k^c(x, Q^2, m_c^2) = 2e_c^2 \frac{\alpha_s(\mu^2)}{2\pi} I_k(x, \mu^2) \times G(x, \mu^2), \quad (9)$$

where

$$I_k(x, \mu^2) = \int_{1-\frac{1}{a}}^{1-x} C_{g,k}^c(1-z, \zeta)(1-z)^{\lambda_g} dz, \quad (10)$$

here $C_{g,k}^c$ is defined by Eq.4. We observe that this equation (Eq.9) is directly dependence to the gluon distribution, which is usually taken from the GRV [16], CETQ [21], MRST [22] parameterizations or DL [3-5] model. In what follows we shall use the gluon distribution with an intercept according to the hard-pomeron behavior at the DL model.

In fact, the gluon distribution function input $G(x, \mu^2)$ does cancel in the ratio of the charm structure functions as we have

$$R^c = \frac{I_L(x, \mu^2)}{I_2(x, \mu^2)}. \quad (11)$$

Therefore, this ratio, which is independent of the gluon distribution function, is very useful for practical applications. In this equation we used the solutions of the NLO BGF analysis and considered λ_g as a hard (Lipatov) Pomeron.

One striking feature of the Pomeron effective exponents to the behavior of the charm structure functions are the predictions of the charm exponents with respect to Eq.9. Namely, the charm exponents λ_k^c at small x are not a function of the variable x . Here we show that the charm structure function exponents exhibit the hard pomeron behavior, where we have taken into account that this behavior is given by the gluon distribution exponent.

Therefore, the concept of the hard pomeron with an intercept that is independent of Q^2 is supported here for the charm structure functions. As we have

$$\lambda_k^c \simeq \lambda_g + \frac{\partial}{\partial \ln \frac{1}{x}} \ln \left[\int_{1-\frac{1}{x}}^{1-x} C_{g,k}^c (1-z, \zeta) (1-z)^{\lambda_g} dz \right]. \quad (12)$$

In this equation, the second term of the right hand Eq.12 at any value of x and all Q^2 values, is very small. We conclude that a simplified power- like parameterization with $\lambda_k^c \simeq \lambda_g$ leads to the violation of unitarity providing the Froisart- Martin [23] bound, at low- x values. We found that our results for the charm structure functions exponents at the renormalization scales are the same hard (Lipatov) pomeron intercept in a wide region of Q^2 and x values. Consequently, these results show that λ_k^c determined within the given errors are constant at small- x . Also, it is a straightforward matter to consider of the logarithmic derivatives of the charm structure functions defined by $\frac{\partial \ln F_k^c(x, Q^2)}{\partial \ln \frac{1}{x}}$ [24]. We note that the charm structure functions exponents, when starting from the Regge- like behavior of the charm structure functions, can be written by

$$\lambda_k^c \simeq \frac{\partial \ln F_k^c(x, Q^2)}{\partial \ln \frac{1}{x}} + \ln(x) \frac{\partial \lambda_k^c}{\partial \ln \frac{1}{x}}. \quad (13)$$

With respect to the charm structure functions (Eq.9), we can define the charm intercepts into the logarithmic x -derivatives of the charm structure functions and the derivatives of the charm intercepts.

Results and Discussion

In this section, we present numerical analysis of the NLO corrections to the charm structure functions. In our calculations, we use the DL parametrization of the gluon distribution and also we set the running coupling constant with $\Lambda = 0.224 \text{ GeV}$, and for our input parameters we choose $m_c = 1.5 \text{ GeV}$. The theoretical uncertainties in our result are according to the renormalization scales $\mu^2 = 4m_c^2$ and $\mu^2 = 4m_c^2 + Q^2$.

Fig.2 shows the quantity $F_2^c(x, Q^2)$ as a function of x for $Q^2 = 45 \text{ GeV}^2$. The LO and NLO predictions are given by the theoretical uncertainty from the renormalization scales, correspondingly. The GJR parameterization [25] are presented by solid curve. One can see that NLO corrections to the BGF kernels are importance, especially for low $x < 0.01$. At the same time, the different between the NLO and LO corrections to the charm structure function increase as x decreases, when compared to the GJR parameterization.

In Figs.3 and 4 we present the behavior of the $F_k^c(k = 2, L)$ charm structure functions as a function of x that accompanied with the theoretical uncertainty, and compared to the ZEUS and H1 data [13]. Also we

compared our results for the charm structure function to the DL model [3-5] (Solid curve) and the color dipole model [26] (Dash curve). We can observe that our results are comparable with the experimental data and also with these models. We can also obtain a reasonable description for the longitudinal charm structure function, when compared results only with the color dipole model [26]. We observed that this corresponding is good at all Q^2 values.

As can be seen in all figures, the increase of our calculations for the charm structure functions $F_k^c(x, Q^2)$ towards low x are consistent with the experimental data. This implies that the x dependence of the charm structure functions at low x are consistent with a power law, $F_k^c = A_k x^{-\lambda_k^c}$, for fixed Q^2 . Having concluded that the data for F_k^c require a hard Pomeron component, as tested this behavior with our results.

In Fig.5 we present our results for the ratio $R^c = F_L^c / F_2^c (= \frac{I_L(x, \mu^2)}{I_2(x, \mu^2)})$ [18,27-28] in charm lepto-production. The theoretical uncertainty in our results related to the renormalization scale choices. We observe that this ratio is independent of x for $x \leq 0.01$ in a wide range of Q^2 . We see that this value is approximately between 0.10 and 0.24 in a region of Q^2 and this prediction for R^c is close to the results Refs.[18,26-29]. In Fig.6 we present the ratio R^c as function of Q^2 at $x = 0.001$ with respect to the theoretical uncertainty. We can see that the behavior of this ratio is agree well with the prediction from Ref.18. As both have a maximum value between $Q^2 = 10$ and 100 GeV^2 and then fall to increase of Q^2 value. These results are in agreement to the k_t - factorization approach [27] only at low Q^2 that it is continues to rise with increasing of Q^2 value. In Fig.7, we show the logarithmic x -derivatives of the charm structure functions. In this figure, we can observe that logarithmic x -derivatives of the charm structure functions are constant at all Q^2 and x values. In fact, it is more likely that x - slope depends very weakly on x and it is not depend on Q^2 . Therefore the Pomeron intercept for the charm structure functions can be defined as $\alpha_P = 1 + \lambda_k^c \simeq 1.44$ and this is according to exchange a hard Pomeron object. Consequently, we can observe that x - slope of the charm structure function exponents ($\frac{\partial \lambda_k^c}{\partial \ln \frac{1}{x}}$) does not depend on x . Therefore the logarithmic x -derivatives of the charm structure functions are equal to the charm- Pomeron intercept as $\lambda_k^c \simeq \frac{\partial \ln F_k^c(x, Q^2)}{\partial \ln \frac{1}{x}}$.

Summary

In conclusion, our numerical results for the charm structure functions at low x are obtained by applying the hard (Lipatov) pomeron behavior at all Q^2 values in the NLO analysis. To confirm the method and results, the calculated values are compared with the H1 and ZEUS

data and other models on the charm structure functions, at small x . This behavior at low x is consistent with a effective power behavior for the charm structure functions ($F_k^c(x, Q^2) = A_k^c x^{-\lambda_k^c}$). We can observed that the charm structure functions increase as usual, as x decreases. The form of the obtained distribution function for the charm structure functions are similar to the predicted from the proton parameterization, and this is in agreement with the increase observed by the H1 and ZEUS experiments. We shown that the ratio $R^c = F_L^c/F_2^c$ for the charm structure functions is constant at low- x and all Q^2 values and its independent of the input gluon distribution function. Results are in agreement with those extracted in Refs.[19,27] within the all uncertainty in the framework of perturbative QCD. We have therefore obtained the charm exponents (λ_k^c) and show that they are equal to the derivative of the charm structure functions as $\partial \ln F_k^c(x, Q^2) / \partial \ln \frac{1}{x} = \lambda_k^c$. This behavior of the charm structure functions at low x is consistent with a power- law behavior and is in agreement with other models (DL and color dipole models).

References

1. Yu.L.Dokshitzer, Sov.Phys.JETP **46**, 641(1977); G.Altarelli and G.Parisi, Nucl.Phys.B **126**, 298(1977); V.N.Gribov and L.N.Lipatov, Sov.J.Nucl.Phys. **15**, 438(1972).
2. A.De Rujula *et al.*, phys.Rev.D **10**, 1649(1974); R.D.Ball and S.Forte, Phys.Lett.B **335**, 77(1994).
3. A.Donnachie and P.V.Landshoff, Z.Phys.C **61**, 139(1994); Phys.Lett.B **518**, 63(2001); Phys.Lett.B **533**, 277(2002); Phys.Lett.B **470**, 243(1999); Phys.Lett.B **550**, 160(2002).
4. R.D.Ball and P.V.landshoff, J.Phys.G**26**, 672(2000).
5. P.V.landshoff, arXiv:hep-ph/0203084 (2002).
6. E.A.Kuraev, L.N.Lipatov and V.S.Fadin, Phys.Lett.B **60**, 50(1975); Sov.Phys.JETP **44**, 433(1976); *ibid.* **45**, 199(1977); Ya.Ya.Balitsky and L.N.Lipatov, Sov.J.Nucl.Phys. **28**, 822(1978).
7. A.Vogt, arXiv:hep-ph:9601352v2(1996).
8. H.L.Lai and W.K.Tung, Z.Phys.C**74**,463(1997).
9. A.Donnachie and P.V.Landshoff, Phys.Lett.B**470**,243(1999).
10. N.Ya.Ivanov, Nucl.Phys.B**814**, 142(2009).
11. F.Carvalho, *et.al.*, Phys.Rev.C**79**, 035211(2009).
12. S.J.Brodsky, P.Hoyer, C.Peterson and N.Sakai,Phys.Lett.B**93**, 451(1980); S.J.Brodsky, C.Peterson and N.Sakai, Phys.Rev.D**23**, 2745(1981).
13. A.V.Kotikov and G.Parente, Phys.Lett.B **379**, 195(1996).
14. K.Lipta, PoS(EPS-HEP)313,(2009).
15. C. Adloff *et al.* [H1 Collaboration], Z. Phys. **C72**, 593 (1996); J. Breitweg *et al.* [ZEUS Collaboration], Phys. Lett. **B407**, 402 (1997); C. Adloff *et al.* [H1 Collaboration], Phys. Lett. **B528**, 199 (2002); S. Aid *et. al.*, [H1 Collaboration], Z. Phys. **C72**, 539 (1996); J. Breitweg *et. al.*, [ZEUS Collaboration], Eur. Phys. J. **C12**, 35 (2000); S. Chekanov *et. al.*, [ZEUS Collaboration], Phys. Rev. **D69**, 012004 (2004); Aktas *et al.* [H1 Collaboration], Eur. Phys.J. **C45**, 23 (2006); F.D. Aaron *et al.* [H1 Collaboration],Phys.Lett.b**665**, 139(2008), Eur.Phys.J.C**65**,89(2010).
16. M.Gluk, E.Reya and A.Vogt, Z.Phys.C**67**, 433(1995); Eur.Phys.J.C**5**, 461(1998).
17. E.Laenen, S.Riemersma, J.Smith and W.L. van Neerven, Nucl.Phys.B **392**, 162(1993).
18. A. Y. Illarionov, B. A. Kniehl and A. V. Kotikov, Phys. Lett. B **663**, 66 (2008).
19. S. Catani, M. Ciafaloni and F. Hautmann, Preprint CERN-Th.6398/92, in Proceeding of the Workshop on Physics at HERA (Hamburg, 1991), Vol. 2., p. 690; S. Catani and F. Hautmann, Nucl. Phys. B **427**, 475(1994); S. Riemersma, J. Smith and W. L. van Neerven, Phys. Lett. B **347**, 143(1995).
20. B.Rezaei and G.R.Boroun, JETP**112**, No.3, 381(2011).
21. H.L.Lai *et. al.*, [CTEQ Collaboration], Eur.Phys.J.C**12**, 375(2000).
22. A.D.Martin, R.G.Roberts, W.J.Stirling and R.S. Thorn, Eur.Phys.J.C**35**, 325(2004).
23. M.Froissart and A.Martin, Nuovo Cim.A**42**, 930(1965).
24. P.Desgrolard *et.al.*, JHEP**02**, 029(2002).
- 25.M. Gluck, P. Jimenez-Delgado, E. Reya, Eur.Phys.J.C**53**,355(2008).
26. N.N.Nikolaev and V.R.Zoller, Phys.Lett. **B509**, 283(2001).
27. A. V. Kotikov, A. V. Lipatov, G. Parente and N. P. Zotov Eur. Phys. J. C **26**, 51 (2002).
28. V. P. Goncalves and M. V. T. Machado, Phys. Rev. Lett. **91**, 202002 (2003).
29. N.Ya.Ivanov, Nucl.Phys.B**814** , 142 (2009).

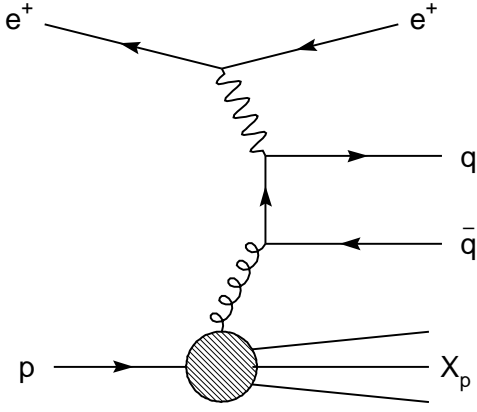


FIG. 1: The photon- gluon fusion

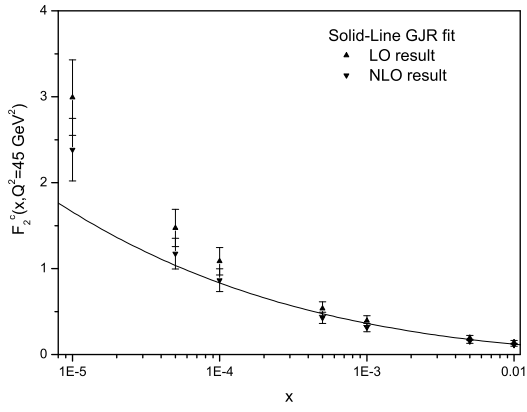


FIG. 2: x dependence of the charm structure function F_2^c at $Q^2 = 45 \text{ GeV}^2$. Plotted are the LO (Up triangle) and NLO (Down triangle) our predictions that accompanied to the errors due to the renormalization scales, as well as the GJR parameterization [25](Solid line) results.

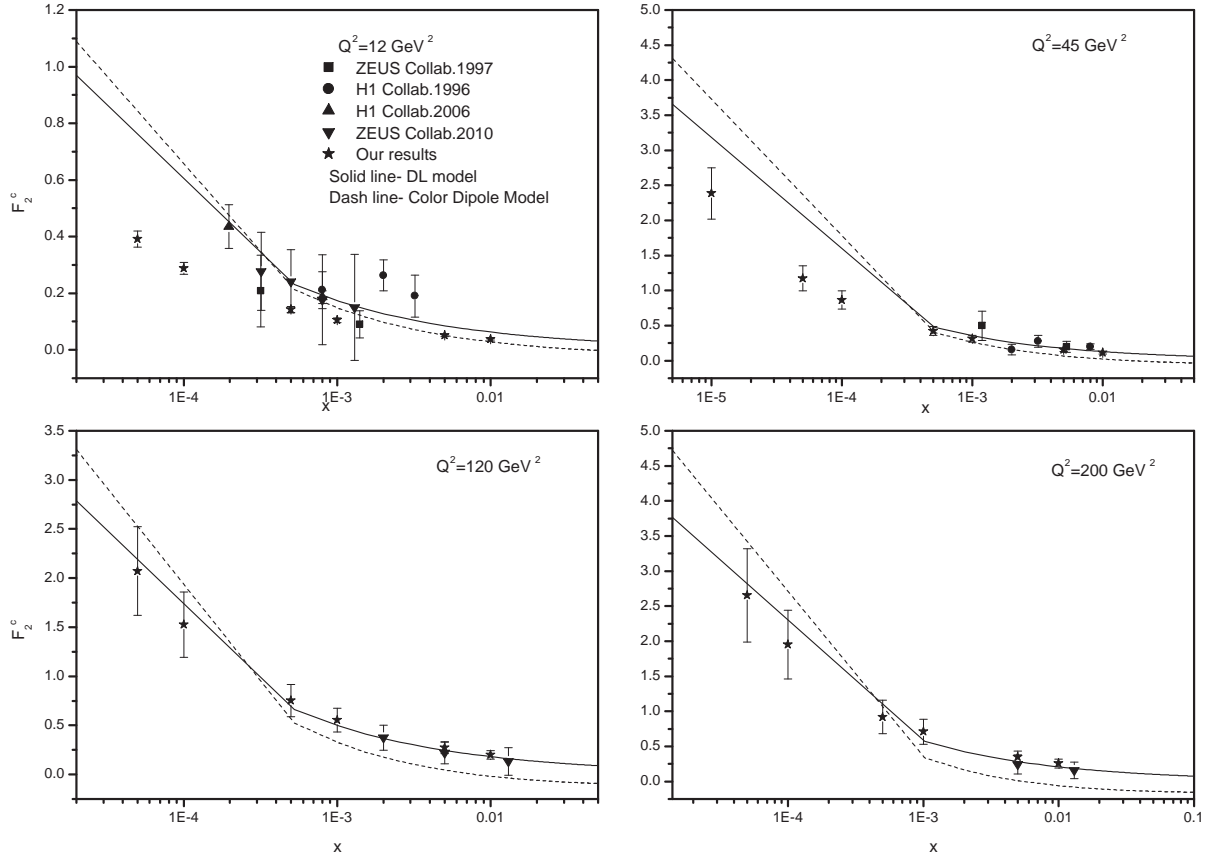


FIG. 3: The charm component of the structure function for different values of Q^2 (12, 45, 120 and 200 GeV^2) as function of x . These results are the NLO predictions that accompanied to the theoretical uncertainty related to the renormalization scales. The solid and dash curves represents F_2^c for DL [3-5] and color dipole [25] models. Data are from H1 and ZEUS Collab. that accompanied to the total errors [15].

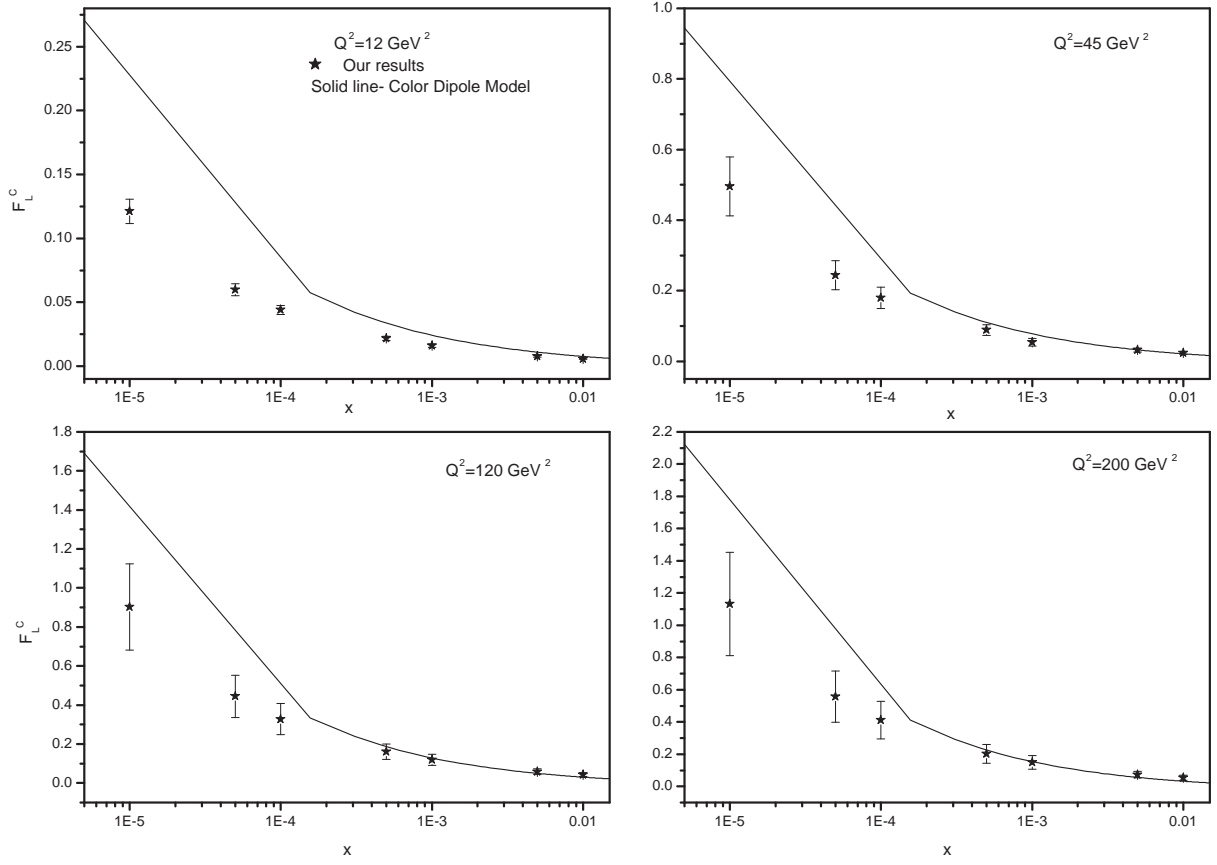


FIG. 4: The charm component of the longitudinal structure function at the Q^2 values 12, 45, 120 and 200 GeV^2 as function of x . These results are the NLO predictions that accompanied to the theoretical uncertainty related to the renormalization scales. The solid curves represents F_L^c from the color dipole [25] model.

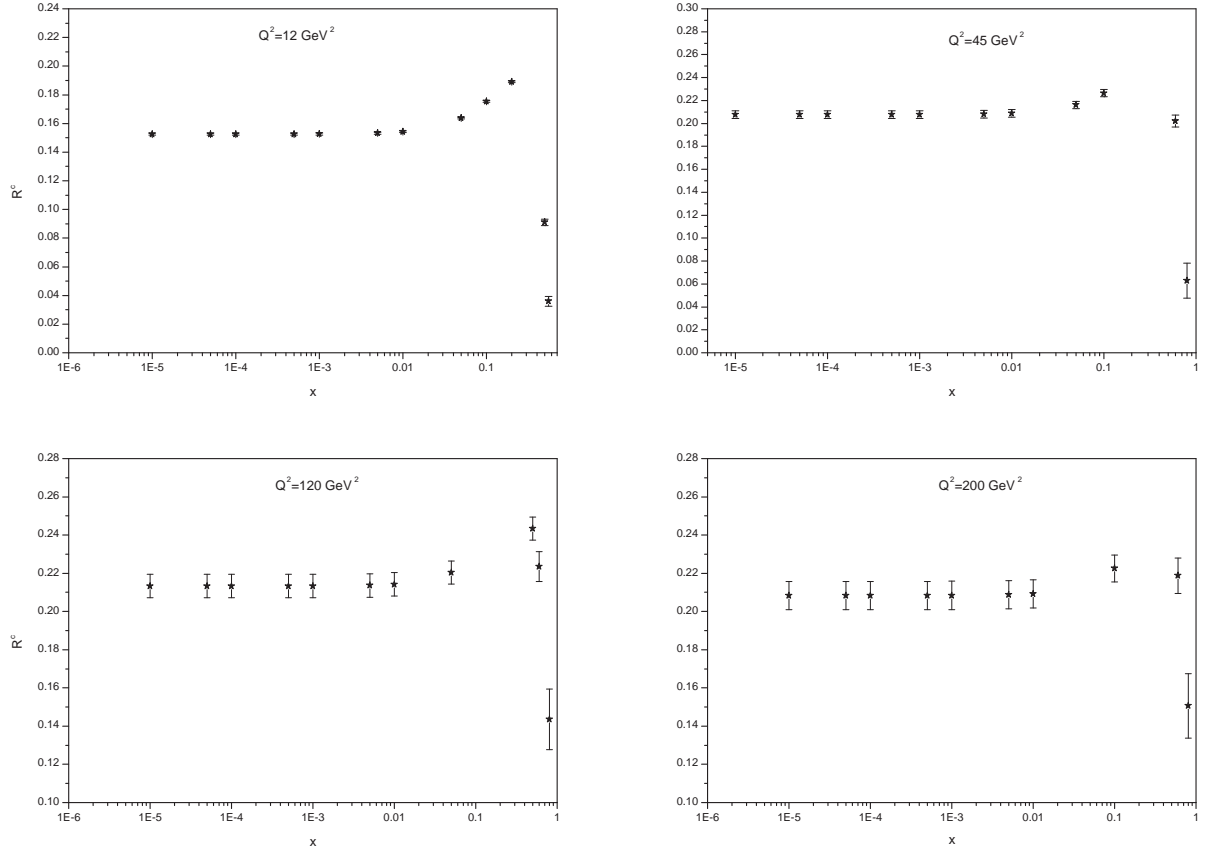


FIG. 5: The ratio $R^c = F_L^c / F_2^c$ as a function of x for different values of Q^2 in NLO analysis.

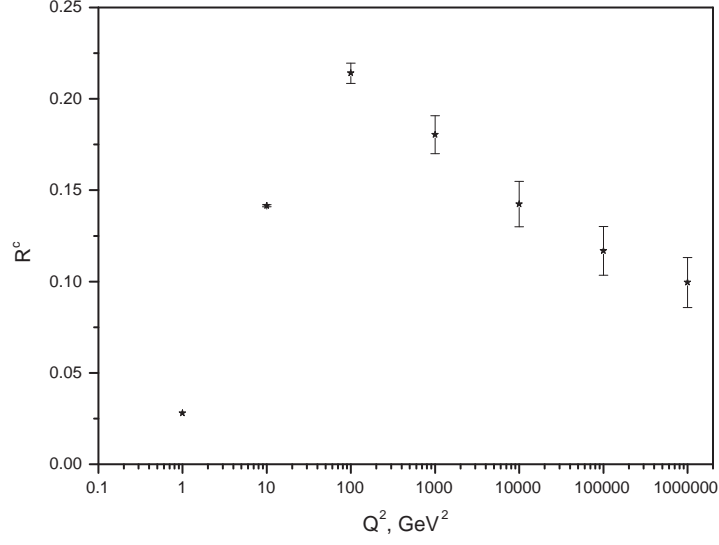


FIG. 6: The ratio $R^c = F_L^c / F_2^c$ as a function of Q^2 at $x = 0.001$ in NLO analysis.

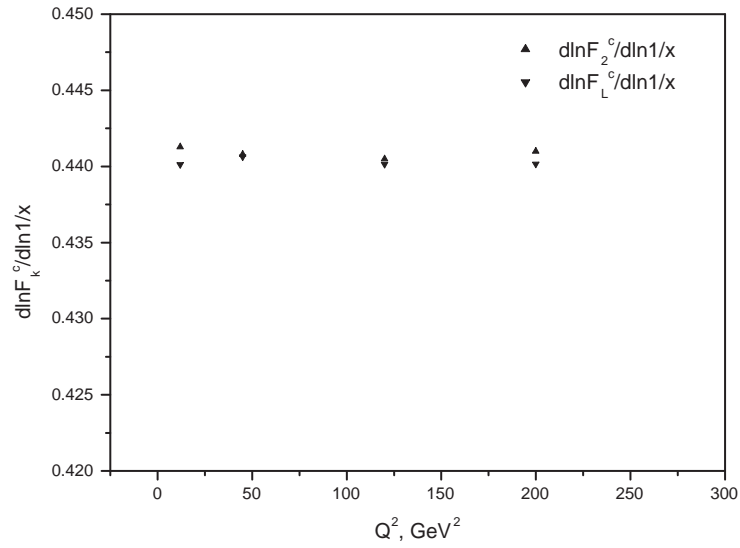


FIG. 7: Logarithmic x -derivatives of the charm structure function $\ln F_k^c(x, Q^2) / \ln \frac{1}{x}$ as function of Q^2 values.